

# Strong intramolecular Dy<sup>III</sup>-Dy<sup>III</sup> magnetic couplings up to 15.00 cm<sup>-1</sup> in phenoxy-bridged dinuclear 4f complexes

Wei Zhang,<sup>a</sup> Shao-Min Xu,<sup>a</sup> Zhao-Xia Zhu,<sup>a</sup> Jing Ru,<sup>\*b</sup> Yi-Quan Zhang<sup>\*c</sup> and Min-Xia Yao<sup>\*a</sup>

<sup>a</sup> College of Chemistry & Molecular Engineering, Nanjing Tech University, Nanjing, 211816, P. R. China.

<sup>b</sup> School of Chemistry and Chemical Engineering, Liaocheng University, Liaocheng, 252059, P. R. China

<sup>c</sup> Jiangsu Key Lab for NSLSCS, School of Physical Science and Technology, Nanjing Normal University, Nanjing 210023, China

**Table S1** Selected bond lengths (Å) and angles (°) for **1-3**.

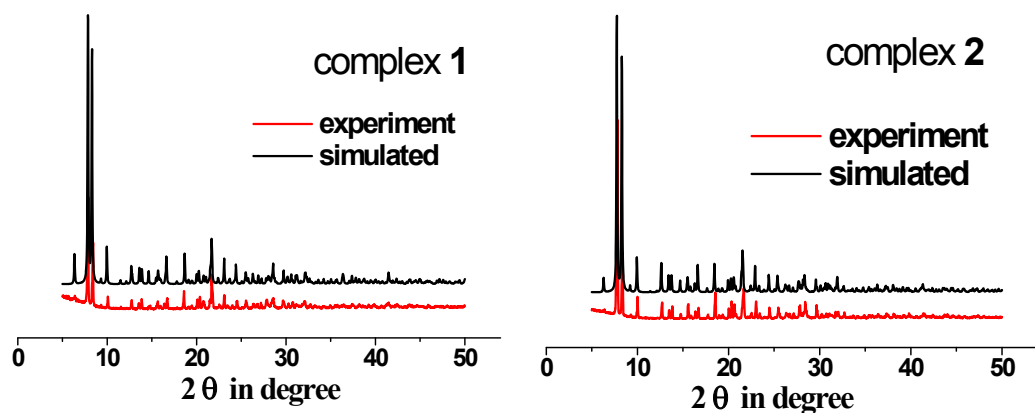
	<b>1</b>	<b>2</b>	<b>3</b>		
Gd(1)-O(1)	2.317(3)	Tb(1)-O(1)	2.304(5)	Dy(1)-O(1)	2.298(6)
Gd(1)-O(2)	2.325(3)	Tb(1)-O(2)	2.306(5)	Dy(1)-O(2)	2.300(6)
Gd(1)-O(3)	2.332(2)	Tb(1)-O(3)	2.320(5)	Dy(1)-O(3)	2.320(6)
Gd(1)-O(4)	2.332(3)	Tb(1)-O(4)	2.322(4)	Dy(1)-O(4)	2.319(6)
Gd(1)-O(6)	2.370(2)	Tb(1)-O(6)	2.357(4)	Dy(1)-O(6)	2.302(6)
Gd(1)-O(6)'	2.332(2)	Tb(1)-O(6)'	2.324(4)	Dy(1)-O(6)'	2.357(5)
Gd(1)-N(1)	2.604(3)	Tb(1)-N(1)	2.593(6)	Dy(1)-N(1)	2.579(8)
Gd(1)-N(2)	2.601(4)	Tb(1)-N(2)	2.605(6)	Dy(1)-N(2)	2.590(9)
O(1)-Gd(1)-O(2)	75.35(10)	O(1)-Tb(1)-O(2)	76.02(17)	O(1)-Dy(1)-O(2)	76.3(2)
O(1)-Gd(1)-O(3)	78.26(9)	O(1)-Tb(1)-O(3)	77.86(17)	O(1)-Dy(1)-O(3)	77.7(2)
O(1)-Gd(1)-O(4)	110.68(9)	O(1)-Tb(1)-O(4)	110.21(16)	O(1)-Dy(1)-O(4)	110.0(2)
O(1)-Gd(1)-O(6)	79.53(9)	O(1)-Tb(1)-O(6)	79.91(16)	O(1)-Dy(1)-O(6)	146.0(2)
O(1)-Gd(1)-O(6)'	145.84(9)	O(1)-Tb(1)-O(6)'	145.86(16)	O(1)-Dy(1)-O(6)'	80.3(2)
O(1)-Gd(1)-N(1)	76.34(10)	O(1)-Tb(1)-N(1)	75.84(16)	O(1)-Dy(1)-N(1)	75.6(2)
O(1)-Gd(1)-N(2)	142.83(10)	O(1)-Tb(1)-N(2)	143.84(18)	O(1)-Dy(1)-N(2)	143.7(3)
O(2)-Gd(1)-O(3)	73.93(9)	O(2)-Tb(1)-O(3)	73.44(16)	O(2)-Dy(1)-O(3)	74.5(2)
O(2)-Gd(1)-O(4)	143.55(9)	O(2)-Tb(1)-O(4)	143.49(16)	O(2)-Dy(1)-O(4)	144.1(2)
O(2)-Gd(1)-O(6)	106.25(9)	O(2)-Tb(1)-O(6)	85.27(16)	O(2)-Dy(1)-O(6)	105.9(2)
O(2)-Gd(1)-O(6)'	85.06(9)	O(2)-Tb(1)-O(6)'	106.73(16)	O(2)-Dy(1)-O(6)'	83.9(2)
O(2)-Gd(1)-N(1)	142.50(10)	O(2)-Tb(1)-N(1)	142.80(17)	O(2)-Dy(1)-N(1)	142.1(2)
O(2)-Gd(1)-N(2)	74.56(11)	O(2)-Tb(1)-N(2)	75.29(18)	O(2)-Dy(1)-N(2)	75.4(3)
O(3)-Gd(1)-O(6)	152.58(9)	O(3)-Tb(1)-O(4)	73.03(15)	O(3)-Dy(1)-O(6)'	152.2(2)

\* To whom correspondence should be addressed. Email: yaomx@njtech.edu.cn; hptx214@163.com; zhangyiquan@njnu.edu.cn Fax: +86-25-58139528.

O(3)-Gd(1)-N(1)	123.07(9)	O(3)-Tb(1)-O(6)	152.26(16)	O(3)-Dy(1)-N(1)	122.7(2)
O(3)-Gd(1)-N(2)	72.85(10)	O(3)-Tb(1)-O(6)'	135.10(16)	O(3)-Dy(1)-N(2)	73.1(3)
O(3)-Gd(1)-O(4)	72.45(9)	O(3)-Tb(1)-N(1)	122.92(17)	O(4)-Dy(1)-O(3)	72.7(2)
O(4)-Gd(1)-O(6)	131.18(9)	O(3)-Tb(1)-N(2)	73.21(18)	O(4)-Dy(1)-O(6)'	131.7(2)
O(4)-Gd(1)-N(1)	70.48(9)	O(4)-Tb(1)-O(6)	131.00(15)	O(4)-Dy(1)-N(1)	70.5(2)
O(4)-Gd(1)-N(2)	82.42(10)	O(4)-Tb(1)-O(6)'	87.98(15)	O(4)-Dy(1)-N(2)	81.5(2)
O(6)-Gd(1)-N(1)	65.95(9)	O(4)-Tb(1)-N(1)	70.22(16)	O(6)-Dy(1)-O(3)	136.1(2)
O(6)-Gd(1)-N(2)	118.73(9)	O(4)-Tb(1)-N(2)	81.61(17)	O(6)-Dy(1)-O(4)	88.2(2)
O(6)'-Gd(1)-O(3)	135.63(9)	O(6)-Tb(1)-N(1)	66.24(16)	O(6)-Dy(1)-O(6)'	66.4(2)
O(6)'-Gd(1)-O(4)	88.47(9)	O(6)-Tb(1)-N(2)	118.85(17)	O(6)-Dy(1)-N(1)	84.5(2)
O(6)'-Gd(1)-O(6)	66.82(11)	O(6)'-Tb(1)-O(6)	66.67(18)	O(6)-Dy(1)-N(2)	65.1(2)
O(6)'-Gd(1)-N(1)	84.47(9)	O(6)'-Tb(1)-N(1)	84.22(16)	O(6)'-Dy(1)-N(1)	66.8(2)
O(6)'-Gd(1)-N(2)	65.02(9)	O(6)'-Tb(1)-N(2)	64.94(17)	O(6)'-Dy(1)-N(2)	118.4(2)
N(1)-Gd(1)-N(2)	139.67(11)	N(1)-Tb(1)-N(2)	138.86(18)	N(1)-Dy(1)-N(2)	139.2(3)

**Table S2** Continuous Shape Measures (CShMs) of the coordination geometry for  $\text{Ln}^{\text{III}}$  ions in compounds **1-3**.

	Complex	CU-8	SAPR-8	TDD-8
	<b>1</b>	9.759	<b>1.410</b>	2.901
	<b>2</b>	9.970	<b>1.384</b>	2.801
	<b>3</b>	9.781	<b>1.353</b>	2.745
CU-8	$\text{O}_\text{h}$	Cube		
SAPR-8	$\text{D}_{4\text{d}}$	Square antiprism		
TDD-8	$\text{D}_{2\text{d}}$	Triangular dodecahedron		



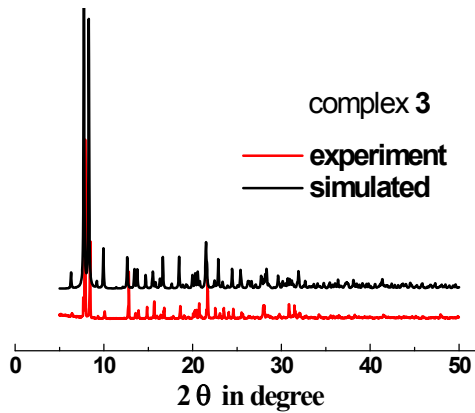


**Fig. S1** PXRD patterns for complexes **1-3**.

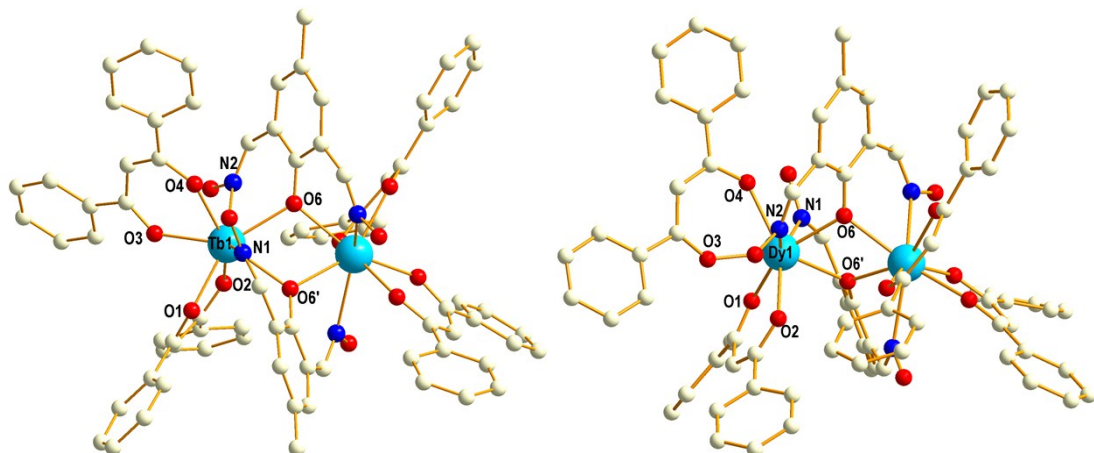


Fig. S2. Molecular structures of  $[\text{Tb}_2(\text{dbm})_2(\text{LH}_2)_2]\cdot\text{H}_2\text{O}$  (**2**, left) and  $[\text{Dy}_2(\text{dbm})_2(\text{LH}_2)_2]\cdot\text{H}_2\text{O}$  (**3**, right). Hydrogen atoms and the solvent water molecules have been omitted for clarity.

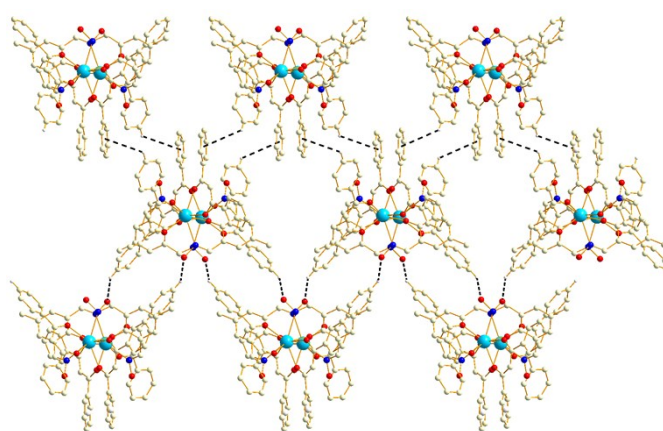


Fig. S3. 2D supramolecular framework of **1** generated by intermolecular C–H···O<sub>oxime</sub> and C–H···π interactions.

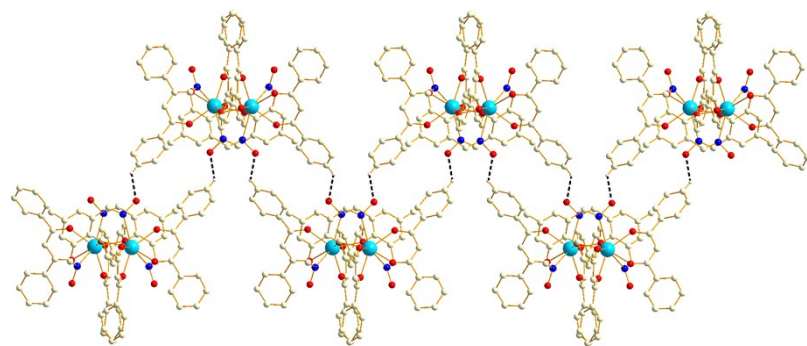


Fig. S4. One-dimensional supramolecular chain of **2** generated by intermolecular C–H $\cdots$ O<sub>oxime</sub> H-bonding interactions.

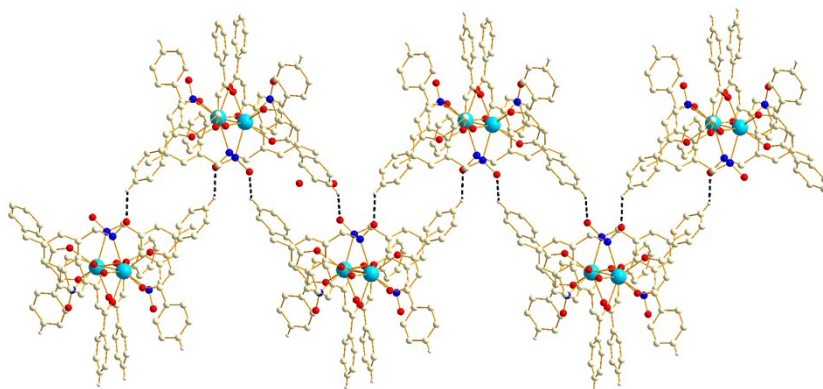
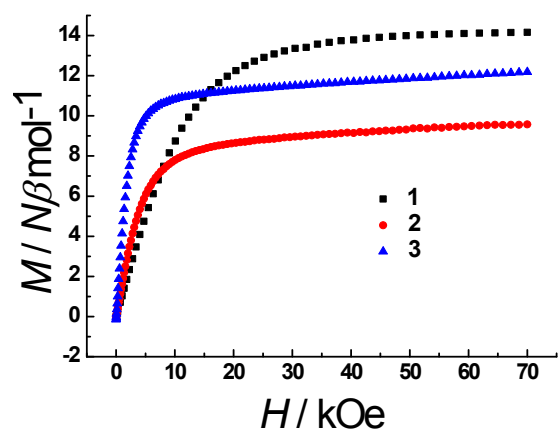
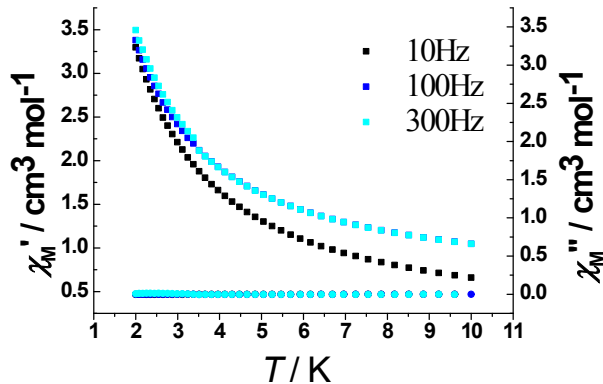


Fig. S5. One-dimensional supramolecular chain of **3** generated by intermolecular C–H $\cdots$ O<sub>oxime</sub> H-bonding interactions.



**Fig. S6** Field dependence of magnetization for **1-3** at 2.0 K



**Fig. S7** Temperature dependence of the in-phase  $\chi'$  and out-of-phase  $\chi''$  at different frequencies in a 3 Oe ac field oscillating at 10–300 Hz with a zero dc field for **2**

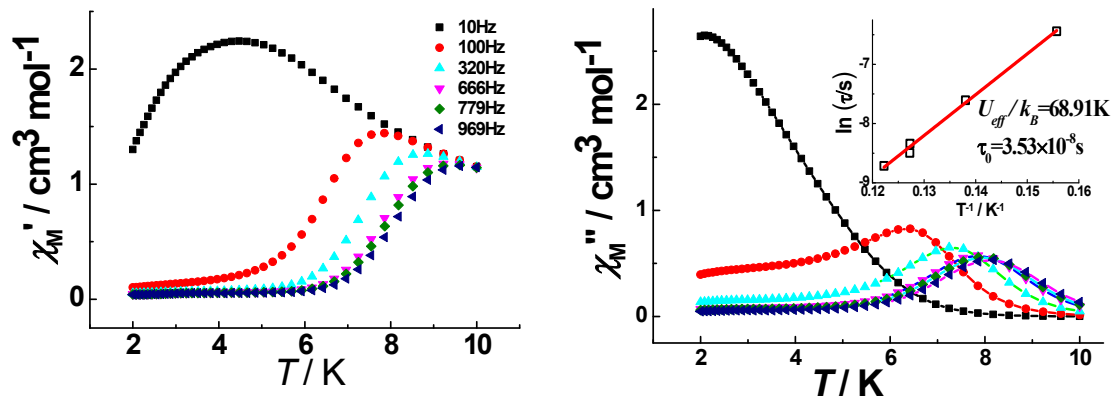


**Fig. S8** Temperature dependence of the in-phase  $\chi'$  and out-of-phase  $\chi''$  at different frequencies in a 3 Oe ac field oscillating at 10–969 Hz with a zero dc field for **3**; Inset: The Arrhenius fits for the  $\ln \tau$  vs  $T^{-1}$  plots from ac- $T$  data of **3**. The red solid line represents the best fits of these data.

## Computational details

Although there is only a crystallographically independent Dy<sup>III</sup> ion in complex **3**, both Dy<sup>III</sup> fragments are calculated. Complete-active-space self-consistent field (CASSCF) calculations on individual Dy<sup>III</sup> fragments indicated as Dy1 and Dy1' (see Fig. S9 for the calculated model structures of Dy1 and Dy1') on the basis of single-crystal X-ray determined geometry have been carried out with MOLCAS 8.4<sup>S1</sup> program package. Each individual Dy<sup>III</sup> fragment was calculated keeping the experimentally determined structure of the corresponding compound while the other Dy<sup>III</sup> ion was replaced by diamagnetic Lu<sup>III</sup>.

The basis sets for all atoms are atomic natural orbitals from the MOLCAS ANO-RCC library: ANO-RCC-VTZP for Dy<sup>III</sup>; VTZ for close N and O; VDZ for distant atoms. The calculations employed the second order Douglas-Kroll-Hess Hamiltonian, where scalar relativistic contractions were taken into account in the basis set and the spin-orbit couplings were handled separately in the restricted active space state interaction (RASSI-SO) procedure. For individual Dy<sup>III</sup> fragment, active electrons in 7 active spaces include all *f* electrons (CAS(9 in 7)) in the CASSCF calculation. To exclude all the doubts, we calculated all the roots in the active space. We have mixed the maximum number of spin-free state which was possible with our hardware (all from 21 sextets, 128 from 224 quadruplets, 130 from 490 doublets). SINGLE\_ANISO<sup>S2</sup> program was used to obtain the energy levels, *g* tensors, *m<sub>J</sub>* values, magnetic axes, *et al.*, based on the above CASSCF/RASSI-SO calculations.

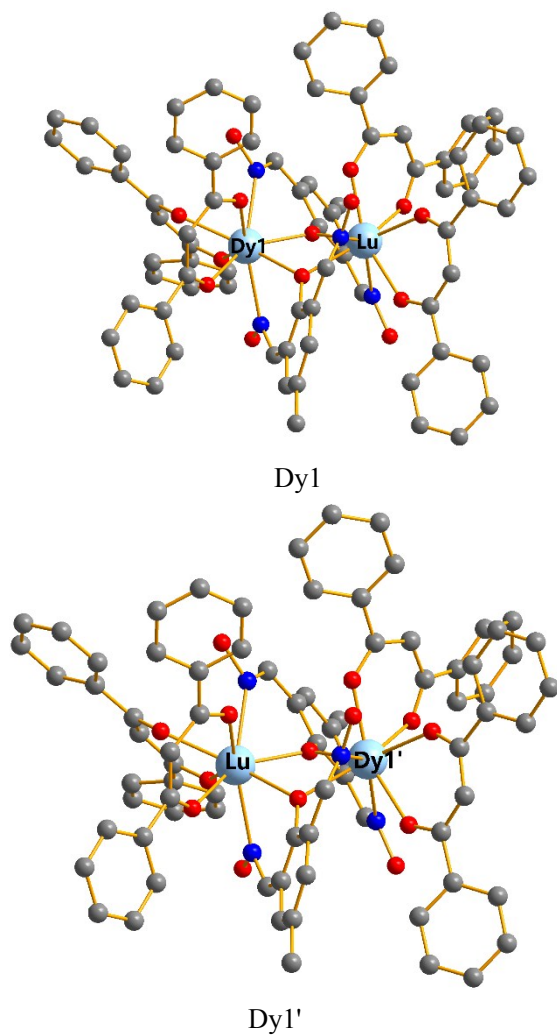


**Fig. S9.** Calculated model structures of Dy1 and Dy1'; H atoms are omitted.

**Table S3.** Calculated energy levels ( $\text{cm}^{-1}$ ),  $g$  ( $g_x$ ,  $g_y$ ,  $g_z$ ) tensors and predominant  $m_J$  values of the lowest eight Kramers doublets (KDs) of Dy1 and Dy1' using CASSCF/RASSI-SO with MOLCAS 8.4.

KDs	$E/\text{cm}^{-1}$	Dy1			Dy1'		
		$g$	$m_J$	$E/\text{cm}^{-1}$	$g$	$m_J$	
1	0.0	0.012			0.013		
		0.022	$\pm 15/2$	0.0	0.022	$\pm 15/2$	
		19.100			19.104		
2	51.9	0.456			0.438		
		0.815	$\pm 13/2$	52.1	0.790	$\pm 13/2$	
		15.578			15.569		
3	74.6	1.255			1.240		
		2.228	$\pm 9/2$	75.0	2.176	$\pm 9/2$	
		12.620			12.622		
4	122.5	5.388			5.372		
		5.935	$\pm 7/2$	123.1	5.905	$\pm 7/2$	
		7.504			7.505		
5	173.5	1.233			1.266		
		2.318	$\pm 3/2$	173.9	2.367	$\pm 3/2$	
		11.513			11.493		
6	246.5	0.233			0.233		
		0.353	$\pm 5/2$	246.9	0.351	$\pm 5/2$	
		14.445			14.454		
7	388.5	0.154			0.154		
		0.243	$\pm 1/2$	389.0	0.245	$\pm 1/2$	
		17.248			17.249		
8	573.5	0.008			0.008		
		0.018	$\pm 11/2$	574.3	0.018	$\pm 11/2$	
		19.331			19.331		

**Table S4.** Wave functions with definite projection of the total moment  $|m_J\rangle$  for the lowest two KDs of individual Dy<sup>III</sup> fragments for Dy1 and Dy1' using CASSCF/RASSI-SO with MOLCAS 8.4.

	$E/\text{cm}^{-1}$	wave functions
Dy1	0.0	87.27% $ \pm 15/2\rangle + 9.50\% \pm 11/2\rangle$
	51.9	53.03% $ \pm 13/2\rangle + 11.20\% \pm 11/2\rangle + 16.42\% \pm 9/2\rangle + 8.04\% \pm 5/2\rangle$
Dy1'	0.0	87.49% $ \pm 15/2\rangle + 9.51\% \pm 11/2\rangle$
	52.1	53.42% $ \pm 13/2\rangle + 11.27\% \pm 11/2\rangle + 16.42\% \pm 9/2\rangle + 7.87\% \pm 5/2\rangle$

To fit the exchange interaction in compound **3**, we took two steps to obtain them. Firstly, we calculated individual Dy<sup>III</sup> fragment using CASSCF/RASSI-SO to obtain the corresponding magnetic properties. Then, the exchange interaction between the

magnetic centers is considered within the Lines model,<sup>S3</sup> while the account of the dipole-dipole magnetic coupling is treated exactly. The Lines model is effective and has been successfully used widely in the research field of *d* and *f*-elements single-molecule magnets.<sup>S4</sup>

The Ising exchange Hamiltonians for **3** is:

$$\hat{H}_{exch} = -J \hat{S}_{\text{Dy1}}^z \hat{S}_{\text{Dy1}}^z \quad (1)$$

The *J* is parameter of the exchange magnetic interaction between Dy<sup>III</sup> ions. The  $\hat{S}_{\text{Dy}}^z = 1/2$  is the ground pseudospin on the Dy<sup>III</sup> sites. The dipolar magnetic coupling can be calculated exactly, while the exchange coupling constants were fitted through comparison of the computed and measured magnetic susceptibility using the POLY\_ANISO program.<sup>S2</sup>

**Table S5.** Exchange energies *E* (cm<sup>-1</sup>), the energy difference between each exchange doublets  $\Delta_t$  (cm<sup>-1</sup>) and the main values of the *g<sub>z</sub>* for the lowest two exchange doublets of **3**.

	<i>E</i>	$\Delta_t$	<i>g<sub>z</sub></i>
1	0.0	$2.3 \times 10^{-6}$	37.485
2	7.0	$5.7 \times 10^{-6}$	7.377

## References:

- S1 F. Aquilante, J. Autschbach, R. K. Carlson, L. F. Chibotaru, M. G. Delcey, L. De Vico, I. Fdez. Galván, N. Ferré, L. M. Frutos, L. Gagliardi, M. Garavelli, A. Giussani, C. E. Hoyer, G. Li Manni, H. Lischka, D. Ma, P. Å. Malmqvist, T. Müller, A. Nenov, M. Olivucci, T. B. Pedersen, D. Peng, F. Plasser, B. Pritchard, M. Reiher, I. Rivalta, I. Schapiro, J. Segarra-Martí, M. Stenrup, D. G. Truhlar, L. Ungur, A. Valentini, S. Vancoillie, V. Veryazov, V. P. Vysotskiy, O. Weingart, F. Zapata, R. Lindh, *J. Comput. Chem.*, 2016, **37**, 506-541.
- S2 (a) L. F. Chibotaru, L. Ungur, A. Soncini, *Angew. Chem. Int. Ed.*, 2008, **47**, 4126-4129. (b) L. Ungur, W. Van den Heuvel, L. F. Chibotaru, *New J. Chem.*, 2009, **33**, 1224-1230. (c) L. F. Chibotaru, L. Ungur, C. Aronica, H. Elmoll, G. Pilet, D. Luneau, *J. Am. Chem. Soc.*, 2008, **130**, 12445-12455.
- S3 M. E. Lines, *J. Chem. Phys.* 1971, **55**, 2977-2984.
- S4 (a) K. C. Mondal, A. Sundt, Y. H. Lan, G. E. Kostakis, O. Waldmann, L. Ungur,

L. F. Chibotaru, C. E. Anson, A. K. Powell, *Angew. Chem. Int. Ed.* 2012, **51**, 7550-7554. (b) S. K. Langley, D. P. Wielechowski, V. Vieru, N. F. Chilton, B. Moubaraki, B. F. Abrahams, L. F. Chibotaru, K. S. Murray, *Angew. Chem. Int. Ed.* 2013, **52**, 12014-12019.